in terms of spherical Bessel functions. The inversion requires some care but is straight forward. The result is

$$f(x, \tau) = x - 2x^{-2} \sum_{n=1}^{\infty} \zeta_n^{-3}(\cos\zeta_n)^{-1}(x\zeta_n\cos x\zeta_n - \sin x\zeta_n)e^{-\zeta_n^2\tau} \quad (6)$$

where ζ_n is the nth positive root of the transcendental equation

$$\zeta = \tan\zeta \quad (7)$$

The first sixteen values of ζ_n are tabulated in Jahnke and Emde.[1] An analytic approximation for ζ_n accurate to 0.1% is given by Kestin and Persen[2] as

$$\zeta_n \doteq \frac{2n+1}{4}\pi + \left[\left(\frac{2n+1}{4}\right)^2\pi^2 - 1\right]^{1/2} \quad (8)$$

Discussion and Results

The first term in Eq. (6) is the steady-state solution (rigid-body rotation), and the summation gives the transient. The reason that the linearized equation (4) gives the correct steady-state solution is, of course, that the neglected terms vanish as $\tau \to \infty$. Equation (6) has been calculated numerically, and the results are shown in Fig. 1. At nondimensional time $\tau = 0.1$, $f(x, \tau)$ has not yet approached closely to the asymptotic value. However, when $\tau = 1$, the value of $f(x, \tau)$ agrees with the steady-state solution to at least five significant digits. Therefore, as was easily surmised by Stewartson and Roberts,[3] the time required for the establishment of rigid-body rotation of the fluid is of order a^2/ν.

It is worth remarking that, even though the equation solved is linear, with the nonlinear terms completely omitted, the solution is still of boundary-layer type in the sense that for small ν, i.e., small τ, the viscous effects are confined to a narrow region adjacent to the wall. This corresponds to the fact that boundary-layer behavior is not so much dependent upon nonlinearity in the differential equations as it is on the smallness of the coefficient that multiplies the most highly differentiated terms (see, for example, Carrier[4]). If δ is defined as the radial distance from the surface at which the circumferential flow has fallen to 1% of its value at the wall (on the same radius), then, for values of $\tau \leq 0.01$,

$$\delta \doteq 3.7a\tau^{1/2} = 3.7(\nu t)^{1/2} \quad (9)$$

Although the present analysis neglects the effect of the secondary flow on the zonal flow field, the viscous torque at the sphere is still expected to be obtained fairly accurately. This follows because the shear stress at $r = a$ depends only on the radial gradient of (w/r) evaluated right at the surface, and in that region the secondary flow is always small since it vanishes right at $r = a$. Integrating the product of shear stress and moment arm over the surface of the sphere, we find that the torque is

$$T = \int_0^{2\pi}\int_0^{\pi} \mu a^4 \left[\frac{\partial}{\partial r}\left(\frac{w}{r}\right)\right]\Bigg|_{r=a} \sin^2\theta \, d\theta d\phi = \frac{16\pi}{3}\mu a^3\Omega \sum_{n=1}^{\infty} e^{-\zeta_n^2 n\tau} \quad (10)$$

For large values of τ, the first term in the summation dominates, and the torque decays exponentially to zero. As $\tau \to 0$, the torque becomes infinite since the motion was started impulsively from rest. The asymptotic expansion of $T(\tau)$ for small τ is†

$$T(\tau) \sim [8(\pi)^{1/2}/3]\mu a^3\Omega\tau^{-1/2} = [8(\pi)^{1/2}/3](\rho\mu)^{1/2}a^4\Omega t^{-1/2} \quad (11)$$

† The author is indebted to F. Ursell, University of Manchester, for pointing this out.

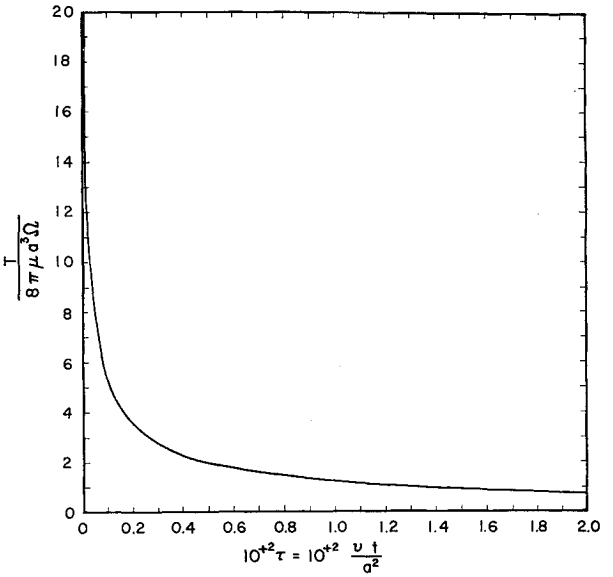

Fig. 2 Nondimensional viscous torque as a function of nondimensional time.

The torque as calculated from Eq. (10) is plotted as a function of time in Fig. 2. It is notable that, in the later stages of flow, the torque, while still significantly different from its asymptotic value of zero, approaches that value very slowly.

References

[1] Jahnke, E. and Emde, F., *Tables of Functions* (Dover Publications, Inc., New York, 1945), 4th ed., p. 30.

[2] Kestin, J. and Persen, L. N., "Small oscillations of bodies of revolution in a viscous fluid," Brown Univ., Providence, R. I., Rept. AF-891/2, p. 36. (October 1954).

[3] Stewartson, K. and Roberts, P. H., "On the motion of a liquid in a spheroidal cavity of a precessing rigid body," J. Fluid Mech. **17**, 1–20 (1963).

[4] Carrier, G. F., "Boundary layer problems in applied mechanics," *Advances in Applied Mechanics* (Academic Press, New York, N. Y., 1953), Vol. III, pp. 1–19.

A Property of Cotangential Elliptical Transfer Orbits

N. X. Vinh*
University of Colorado, Boulder, Colo.

I. Introduction

COTANGENTIAL transfer between two planar, confocal, noncoaxial ellipses has been investigated by many authors. The purpose of this paper is to prove that generally this type of transfer does not yield a minimum energy transfer. Also it will be shown that between two coplanar, confocal, noncoaxial ellipses, there exist two cotangential transfer orbits that yield a relative optimum transfer. One of these two orbits, in the special case of two coaxial terminal ellipses, turns out to be the well-known coapsidal, absolute optimum two-impulses transfer. A practical application of this property is in the case where one or both of the terminal ellipses are almost circular.

Received June 4, 1964; revision received June 18, 1964. This work is supported by ARPA-ARO Contract No. DA-31-124-ARO(D)-139.

* Colonel, Chief of Staff (1957–1962), Vietnamese Air Force; now Graduate Fellow, Department of Aerospace Engineering Sciences.

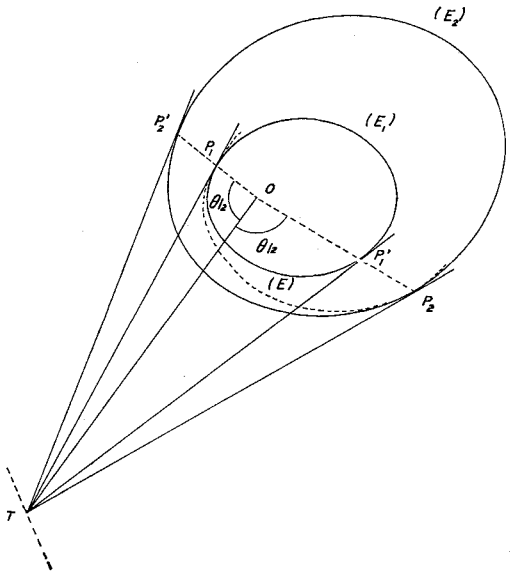

Fig. 1 Geometry of the cotangential transfer ellipse.

II. Geometrical Study of the Transfer Ellipse

A. Construction of the transfer ellipse

Let (E_1) and (E_2) be the terminal ellipses and P_1 and P_2 be the transfer positions. Let (E) be the transfer ellipse. The tangents to (E_1) and (E) at P_1 and to (E_2) and (E) at P_2 intersect each other at a point T (Fig. 1). By a theorem in conic sections, the straight line OT, where O is the common focus, bisects the angle P_1OP_2. From the point T we draw a second tangent TP_2' to the ellipse (E_2). By the same theorem, OT bisects the angle $P_2'OP_2$. Hence, the points O,P_1,P_2' are aligned. Also, if TP_1' is the second tangent drawn from the point T to the ellipse (E_1), the three points O, P_1', P_2 are aligned.

Therefore, given the initial position P_1, to construct the point P_2, first we draw the straight line OP_1P_2'. Then we construct the tangents P_1T and $P_2'T$ intersecting each other at T. From T we can draw the tangent TP_2 to the ellipse (E_2). The cotangential transfer ellipse (E) passing through P_1 and P_2 is then uniquely determined.

It can be shown by geometry that the preceding constructions can be made using only straight edge and compass. Also, when P_1 moves on (E_1), the locus of T is a straight line. The pair of points P_1 and P_2 is defined as of class (T).

B. Velocity from point to point

Consider two points P_1 and P_2 in a Newtonian force field. It is known[1] that the terminus of the required velocity $\mathbf{V}_1$ at P_1 for the vehicle to pass through P_2 is a branch of hyperbola (H_1), having OP_1 and P_1P_2 as asymptotes (Fig. 2). Let V_1^* be the minimum speed from P_1 to P_2:

$$V_1^* = \left[\frac{2\mu}{r_1}\frac{D+d}{D+r_1+r_2}\right]^{1/2} \tag{1}$$

where D is the distance P_1P_2

$$D = (r_1^2 + r_2^2 - 2\,r_1r_2\cos\theta)^{1/2} \tag{2}$$

$$d = r_2 - r_1 \tag{3}$$

Let ϵ_1 be the angle between $\mathbf{V}_1^*$ and $\mathbf{V}_1$; the polar equation of the hyperbola (H_1) is

$$V_1^2 = \frac{2\mu\, r_2(1-\cos\theta)}{r_1(r_1 - r_2\cos\theta + D\cos 2\,\epsilon_1)} \tag{4}$$

Similarly, we have another hyperbola (H_2) at P_2, and since the speed along the trajectory is the same in either direction, we will consider the hyperbola (H_2) as if the vehicle goes from P_2 to P_1.

The polar equation of this hyperbola is

$$V_2^2 = \frac{2\mu\, r_1\,(1-\cos\theta)}{r_2(r_2 - r_1\cos\theta + D\cos 2\,\epsilon_2)} \tag{5}$$

Also it is a known fact that the locus of the second focus of the transfer ellipse is a hyperbola (H) having P_1 and P_2 as foci and transverse axis $d = r_2 - r_1$.

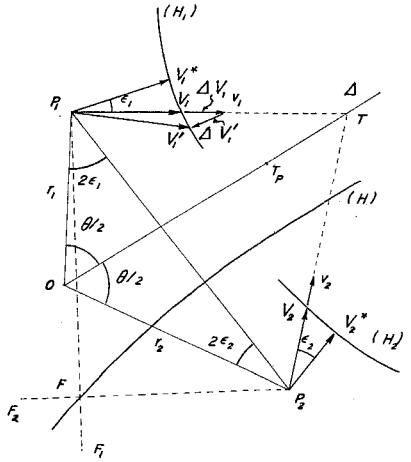

Fig. 2 Geometry of the transfer velocities.

III. Analysis of the Cotangential Transfer

Since we need only to prove that the cotangential transfer, in general, does not yield a minimum energy transfer, without loss of generality we can assume that the terminal points P_1 and P_2 are given first. Then we construct the terminal orbits (E_1) and (E_2) so that P_1 and P_2 are of class (T).

Consider Fig. 2, where P_1 and P_2 are two given points in a Newtonian force field with center of attraction at O. Let $O\Delta$ be the bisector of the angle P_1OP_2. Since P_1 and P_2 are given, the hyperbola (H) and the portions of the hyperbolas (H_1) and (H_2) are completely determined.

To fix the terminal ellipses (E_1) and (E_2) we need only to specify the velocity $\mathbf{v}_1$ and $\mathbf{v}_2$ along (E_1) and (E_2), respectively, at P_1 and P_2. Let $\mathbf{v}_1$ be given first. If (E) is the cotangential transfer ellipse and $\mathbf{V}_1$ is the velocity along (E) at P_1, the direction of $\mathbf{v}_1$ determines completely (E), i.e., $\mathbf{V}_1$, $\mathbf{V}_2$ and F,F being the second focus of (E). By the cotangential requirement, the ellipse (E_2) now can be fixed using only them agnitude of $\mathbf{v}_2$, since the direction of $\mathbf{v}_2$ is determined by $\mathbf{v}_1$ using the construction mentioned in the preceding section. Assume that we have

$$v_1 > V_1 \qquad v_2 > V_2$$

that is,

$$a_1 > a \qquad a_2 > a$$

The total impulse velocities for the cotangential transfer is

$$\sum_T \Delta V = (v_1 - V_1) + (v_2 - V_2) = \Delta V_1 + \Delta V_2$$

By increasing ϵ_1, we modified the transfer ellipse, which is not cotangential now, and the point T is approaching T_P, the limiting position of T for parabolic flight path. Hence, ϵ_2 is also increasing. V_1 and V_2 are increasing and become V_1' and V_2'. It is clear, and it can be proved analytically by considering the distance from a point to a hyperbola, that for small variation of ϵ_1 and ϵ_2

$$\Delta V_1' < \Delta V_1 \text{ and } \Delta V_2' < \Delta V_2$$

Hence, the cotangential transfer does not yield the optimum transfer. If both a_1 and a_2 are less than a, we have the same conclusion by decreasing ϵ_1 and ϵ_2. The assumptions on the

semimajor axis a of the transfer orbit made previously correspond to the case of intersecting terminal ellipses.[2]

For the case where a is between a_1 and a_2, i.e., the terminal ellipses are nonintersecting, we cannot conclude a posteriori, but there exists one case of interest where the cotangential transfer yields a relative minimum energy transfer: that is the case where $\mathbf{v}_1$ is normal to the hyperbola (H_1), i.e., $\mathbf{v}_1$ is colinear to $\mathbf{V}_1$*. By the cotangential requirement, $\mathbf{v}_2$ is also colinear to $\mathbf{V}_2$*. Geometrically, it means that the foci F, F_1, F_2 are on the straight line P_1P_2.

Therefore, given two terminal ellipses (E_1) and (E_2), we can easily construct the transfer terminal points P_1 and P_2 which yield a relative minimum energy transfer by drawing the straight line F_1F_2 where F_1 and F_2 are, respectively, the second foci of (E_1) and (E_2). This straight line intersects (E_1) at P_1 and P_1' and (E_2) at P_2 and P_2'. This gives a couple of transfer ellipses (E_A) and (E_B) (Fig. 3).

For this transfer to be really a minimum, we must have the conditions

$$v_1 \leqslant v_{1_c} \tag{6}$$

$$v_2 \leqslant v_{2_c} \tag{7}$$

where c corresponds to the center of curvature of the hyperbolas (H_1) and (H_2) at their vertices. By carrying out the calculation, using the polar equations (4) and (5), conditions (6) and (7) can be written as

$$\frac{1}{a_1} \geqslant \frac{2}{r_1}\left[1 - \frac{D + r_2 - r_1}{D + r_1 + r_2}\frac{4D^2}{(D - r_1 + r_2\cos\theta)^2}\right] \tag{8}$$

and

$$\frac{1}{a_2} \geqslant \frac{2}{r_2}\left[1 - \frac{D + r_1 - r_2}{D + r_1 + r_2}\frac{4D^2}{(D - r_2 + r_1\cos\theta)^2}\right] \tag{9}$$

Therefore, we can formulate this property as follows: Given two coplanar, confocal, terminal ellipses, there exists two cotangential transfer ellipses that yield a relative minimum energy transfer if conditions (8) and (9) are satisfied. The terminal points of these transfer orbits are aligned with the second foci of the terminal ellipses.

IV. Special Cases of Interest

For the special cases where (E_1) and/or (E_2) are circles, and also for the case where (E_1) and (E_2) are coaxial ellipses, it has been shown that[3] one of these two transfers yields the absolute minimum energy two-impulses transfer. Note that, in these cases, (H_1) and (H_2) are straight lines, and Eqs. (8) and (9) are always satisfied.

For the general case, a practical application of this type of transfer is when one or both terminal ellipses (E_1) and (E_2) have small eccentricities. The first case occurs on a transfer from a low-altitude, nearly circular parking orbit to a high-altitude, elliptical orbit. The second case occurs on interplanetary flight. Under this small-eccentricities assumption, even when the terminal ellipses are noncoaxial, the terminal conditions vary little from the coapsidal transfer conditions. The property of cotangential transfer proved in Sec. III guarantees a relative optimum transfer by cotangential thrusts application. For most practical cases, we can assume that

$$c_2 > c_1 \tag{10}$$

$$a_2 - c_2 > a_1 + c_1 \tag{11}$$

i.e., (E_1) is completely inside of (E_2) regardless of the orientation angle φ, and at least the inner ellipse has small eccentricity.

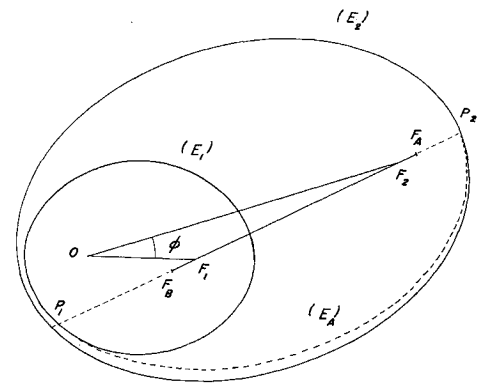

Fig. 3 Aligned foci cotangential transfer ellipse.

Following are the elements of the transfer ellipse (E_A), which is likely the more economical since it is degenerated from the coapsidal transfer ellipse when we rotate (E_2) an angle φ from (E_1). Taking as line of reference the axis of the ellipse (E_1), and letting the distance $F_1F_2 = 2x$ be an alternate parameter, we have

$$x = (c_1^2 + c_2^2 - 2\,c_1c_2\cos\varphi)^{1/2} \tag{12}$$

$$0 \leqslant \varphi \leqslant \pi \tag{13}$$

$$c_2 - c_1 \leqslant x \leqslant c_1 + c_2$$

Major Axis

$$2a = a_1 + a_2 + x \tag{14}$$

Linear Eccentricity

$$2c = \left[\frac{-x^3 + [(a_1 - a_2)^2 + 2(c_1^2 + c_2^2)]\,x + 2(a_1 - a_2)(c_1^2 - c_2^2)}{x}\right]^{1/2} \tag{15}$$

Hence, the eccentricity

$$e = c/a \tag{16}$$

and semilatus rectum

$$p = \frac{x^3 + (a_1 + a_2)\,x^2 + (2a_1a_2 - c_1^2 - c_2^2)x - (a_1 - a_2)(c_1^2 - c_2^2)}{x(a_1 + a_2 + x)} \tag{17}$$

Orientation Angle

$$\tan\varphi_A = \frac{(a_2 - a_1 + x)\,[(c_1 + c_2 + x)(c_1 + c_2 - x)(c_1 - c_2 + x)\,(-c_1 + c_2 + x)\,]^{1/2}}{4c_1^2x + (a_2 - a_1 + x)(c_2^2 - c_1^2 - x^2)} \tag{18}$$

Radial Distance to Terminal Points

$$r_i = 2(p - p_i)/[a_ip - ap_i] \qquad i = 1,2 \tag{19}$$

Thus, when the elements of the terminal ellipses a_i, c_i and the angle φ are known, the elements of the transfer ellipse and the coordinates of the points of transfer together with the required transfer energy can be calculated by the preceding equations.

It is trivial that the equations in this section give the elements of the coapsidal transfer when $c_1 = 0$, or when $\varphi = 0$ or $\varphi = \pi$. (It would be of interest to compare numerically the type of transfer presented in this paper with the approximate solutions for the optimum cotangential transfer derived by Lawden and Smith.[4,5])

References

[1] Battin, R. H., *Astronautical Guidance* (McGraw-Hill Book Co., Inc., New York, 1964), p. 106.

[2] Wen, L.-S., "A study of cotangential, elliptical transfer orbits in space flight," J. Aerospace Sci. 28, 411–416 (1961).
[3] Lawden, D. F., "Impulsive transfer between elliptical orbits," *Optimization Techniques* (Academic Press, New York, 1962), pp. 323–351.
[4] Lawden, D. F., "Optimal transfer via tangential ellipses," J. Brit. Interplanet. Soc. 11, 278–289 (November 1952).
[5] Smith, G. C., "The calculation of minimal orbits," Astronaut. Acta 5, Fasc. 5, 253–265 (1959).

Vibrational Relaxation in Air

DONALD R. WHITE* AND ROGER C. MILLIKAN†
General Electric Company, Schenectady, N. Y.

A LARGE amount of data is now available on the vibrational relaxation of simple systems, that is, the probability of excitation of a diatomic molecule by translation-to-vibration (T-V) energy conversion in a collision with an atom, a like molecule, or some other unexcited diatomic molecule. However, several systems of interest, O_2-H_2, N_2-O_2, and CO-O_2, consist of mixtures of diatomic gases in which the second component is more rapidly excited than the first. The possibility must then be considered that the first species relaxes not only by the simple T-V process but also by the exchange of vibrational energy (V-V process) in a collision with excited molecules of the second species. This note presents data on one such mixture of particular importance, namely, air.

Vibrational relaxation in air has been studied using the same techniques as employed in previous studies of nitrogen[1] and oxygen,[2] i.e., optical interferometry and infrared emission

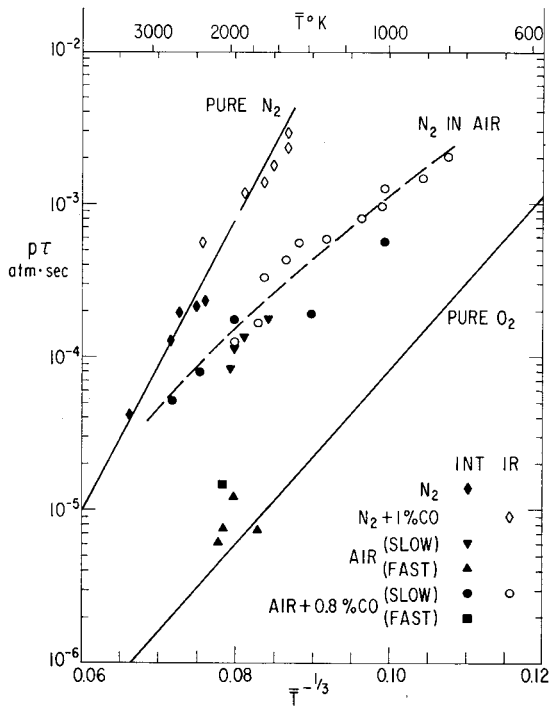

Fig. 1 Experimental data on vibrational relaxation of the components of air.

Received June 11, 1964. This work was supported in part by the Ballistic Systems Division of the U. S. Air Force under Contract AF 04-(694)-222.

* Physicist, General Electric Research Laboratory; also Adjunct Professor of Aeronautics and Astronautics, Rensselaer Polytechnic Institute, Troy, N. Y.
† Physical Chemist, General Electric Research Laboratory.

near 4.6 μ from small amounts of CO added to the test gas. The work falls into two portions, first an extension of our previously reported studies of N_2, and then a study of synthetic air (no CO_2, H_2O, etc.).

Additional data points were taken on the vibrational relaxation of N_2 for two reasons. In the earlier work,[1] relatively few experiments in pure N_2 were included, and those experiments at lower temperatures utilized 5% CO as a tracer for the vibrational state of N_2. If either N_2 or CO were anomalously effective (in the sense of the correlation given in Ref. 3) as a collision partner in exciting the other, then conceivably the small amount of CO could result in an acceleration of the rate of vibrational excitation of N_2, an effect Gaydon and Hurle[4] consider that they may have seen, although alternative explanations are available.

The N_2 line on Fig. 1 for $T^{-1/3} < 0.08$ is taken from Ref. 1, and new points are shown by the diamonds. Solid diamonds are interferometer data on pure N_2, and open diamonds are derived as in Ref. 1 from infrared (IR) emission from a 0.99 N_2 + 0.01 CO mixture. These data provide additional confirmation for the results of Ref. 1 as contrasted to the earlier low-temperature data[5–8] on N_2, extend the shock tube experimental data below 1500°K, and further validate the use of CO as a tracer for following the vibrational excitation of N_2. Recent sodium-line-reversal studies by Hurle[9] extending down to 1700°K also yield N_2 vibration relaxation times in agreement with these data.

To study the vibrational relaxation of air, two mixtures were employed. The first was 0.782 N_2 + 0.21 O_2 + 0.008 CO, and the second had N_2 and O_2 in the same proportions without CO. In the second mixture, only interferometer data can be obtained, and a portion of an interferogram is shown in Fig. 2. In the analysis of the interferograms by Blackman's method,[5] the logarithm of the difference between the observed and the final equilibrium density (δ on Fig. 3) is plotted as a function of distance behind the shock wave. In earlier studies of pure gases and simple mixtures, such a plot has been found to produce a straight line, corresponding to an exponential approach of the shocked gas density to the equilibrium value. For air, however, as indicated by the analysis in Fig. 3 of the record shown in Fig. 2, this is not the case. Here the plot of logδ may be represented as a sum of two straight lines, a slow (solid line) component obtained by fitting a line to the data relatively far behind the shock, and a fast (dashed line) component obtained as the difference between this first line extended forward toward the shock and the observed value of δ. The observed density profile may be interpreted approximately as due to a rapid relaxation of O_2 followed by a relatively slow relaxation of N_2. The large difference in the two relaxation times has led us to reduce the data as though the two processes could be separated. Shock Hugoniots have been calculated for shocked gas state a, assuming no vibrational excitation; for state b, assuming excitation only of O_2; and for

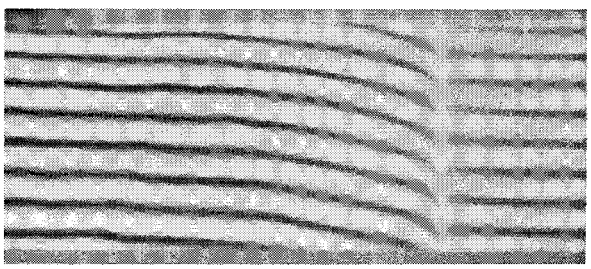

Fig. 2 Interferogram of a Mach 5.13 shock wave traveling to the right into 0.1 atm of air. A density increase displaces the interference fringes upward. The vertical field of view is 2.7 cm and includes the upper surface of the shock tube. The sharper fringe curvature immediately behind the shock front is attributed to vibrational relaxation of O_2.